NAA-SR-3481
METALLURGY AND CERAMICS
40 PAGES

HIGH-STRENGTH ZIRCONIUM ALLOYS

By
R. K. WAGNER
H. E. KLINE

ATOMICS INTERNATIONAL
A DIVISION OF NORTH AMERICAN AVIATION, INC.
P.O. BOX 309 CANOGA PARK, CALIFORNIA

CONTRACT: AT(11-1)-GEN-8
ISSUED: JUL 15 1959

DISCLAIMER

DISTRIBUTION

This report has been distributed according to the category "Metallurgy and Ceramics" as given in "Standard Distribution Lists for Unclassified Scientific and Technical Reports" TID-4500 (14th Ed.), October 1, 1958. A Total of 605 copies was printed.

ACKNOWLEDGMENT

Thanks are due to: Dr. R. L. Eichelberger for the corrosion data; L. C. Metcalf for the mechanical testing; and Mrs. R. E. Selsor for the metallographic studies.

CONTENTS

TABLES

FIGURES

ABSTRACT

The purpose of this program was to investigate the properties of zirconium alloyed with aluminum, tin, and molybdenum.

Using reactor-grade zirconium sponge, 11 zirconium-base alloys were double arc-melted and cast into 6-in.-dia ingots weighting 35 lb each. By such standard hot working procedures as extruding and rolling, the ingots were converted to 1/8-in.-thick strips.

The extruded and rolled products were used for a variety of evaluation studies which included corrosion, thermal conductivity, tensile, and creep tests. The alloys demonstrated short-time elevated temperature strength properties equal to or greater than type-304 stainless steel. Their corrosion resistance in sodium, at 1000°F, compares favorable with that of unalloyed zirconium. The creep resistance and the thermal conductivity were found to be less than those for type-304 stainless steel, but adequate for nuclear reactor application.

I. INTRODUCTION

The use of zirconium and the Zircaloys as fuel-cladding materials for nuclear reactors has been recognized for some time. Characteristics which make these materials suitable for the reactor designer include their: a) low absorption cross-section for thermal neutrons, b) compatibility with uranium and its alloys, and with uranium refractories, and c) compatibility with coolants such as sodium and pressurized water.

Perhaps the greatest disadvantage of these materials is their lack of strength at temperatures in excess of 900°F. This does not present a serious problem in pressurized water reactors, since their operating temperatures are about 600°F. However, in the Sodium Reactor Experiment at Atomics International, the normal operating temperatures of the core are in excess of 900°F, and it is expected that as technological improvements are made on this reactor type, consideration will be given to the use of higher temperatures for increased efficiency.

At the present time, the metal fuel slugs of the SRE are contained in a 0.790-in.-dia by 0.010-in.-wall AISI type-304 stainless steel tube, and are thermally bonded with a 0.010-in. NaK annulus. Because stainless steel has a high absorption cross-section for thermal neutrons, the substitution of a high temperature zirconium-base alloy can effect a considerable saving in neutrons.

The purpose of this work was to develop a zirconium-base alloy which would exhibit properties suitable for use as a fuel cladding material in a sodium-cooled, graphite-moderated reactor. Specifically, the alloy should exhibit:

a) High strength at elevated temperatures

b) Compatibility with sodium and fuel materials

c) Low absorption cross-section for thermal neutrons

d) Relative ease of fabrication

e) Moderate to low cost.

A survey of the literature[1, 2, 3, 4] indicated that several alloying elements of low cross-section could be used to increase both the room temperature and elevated temperature strength of zirconium. Aluminum and tin were chosen as alloying additions for this development work because of their availability and

relatively low cost in the pure state. These elements are peritectoid formers and markedly increase the alpha ⟶ beta transformation temperature. Despite its relatively high cross-section, molybdenum, a eutectoid former, was considered as an alloy addition to improve the hot workability of the peritectoid alloys, and to impart creep resistance in the temperature range of interest.

II. PREPARATION, PROCESS, AND FABRICATION OF THE ZIRCONIUM ALLOYS

A. NOMINAL COMPOSITION

As indicated by the alloy compositions tabulated in Table I, aluminum was used as the major alloying element. To evaluate the effect of additional alloying elements on the properties of the basic zirconium-aluminum binary compositions, tin and molybdenum additions were made.

TABLE I

ZIRCONIUM BASE ALLOYS - NOMINAL COMPOSITION (in wt %)

Alloy No.	Aluminum	Tin	Molybdenum	Zirconium
1	-	-	-	100
2	1.5	-	-	Bal
3	1.5	1.5	-	Bal
4	1.5	3.0	-	Bal
5	1.5	-	1.5	Bal
6	1.5	1.5	1.5	Bal
7	3.0	-	-	Bal
8	3.0	1.5	-	Bal
9	3.0	3.0	-	Bal
10	3.0	1.5	1.5	Bal
11	2	-	-	Bal

B. RAW MATERIAL

The zirconium alloys used in the program were prepared from the raw materials described in Table II. Chemical analysis for the reactor grade

zirconium sponge is included in Table III, and represents both chemical and spectrographic determinations.

TABLE II

RAW MATERIALS

Metal	Form	Purity
Zirconium	Sponge	See TABLE III
Aluminum	Shot	99.9
Tin	Shot	99.9
Molybdenum	Powder	99. +

TABLE III

CHEMICAL ANALYSIS - ZIRCONIUM SPONGE-BLEND 59*

(Analysis in PPM)

CHEMICAL

C	Cl	Fe	Mg	N_2
65	700	700	470	35

SPECTROGRAPHIC

Hf	Al	B	Co	Cr	Cu	Fe	Mg	Mn	Ni	Pb	Si	Ti	V	Mo
40	46	<0.2	<5	100	<20	850	600	25	<10	10	50	30	<20	10

* Hardness: BHN 144.

The raw materials were pressed into 1-1/2-in. -square by 36-in. -long electrodes of a composition corresponding to the nominal analyses described in Table I. Alloy additions, in the forms described in Table II, were made prior to pressing the electrodes. Representative compacted electrodes are shown in Figure1.

C. MELTING

The compacted electrodes were arc-melted, under an argon cover gas at a pressure of ~25 in. of mercury, to produce the first melt 4-in. -dia ingots, one

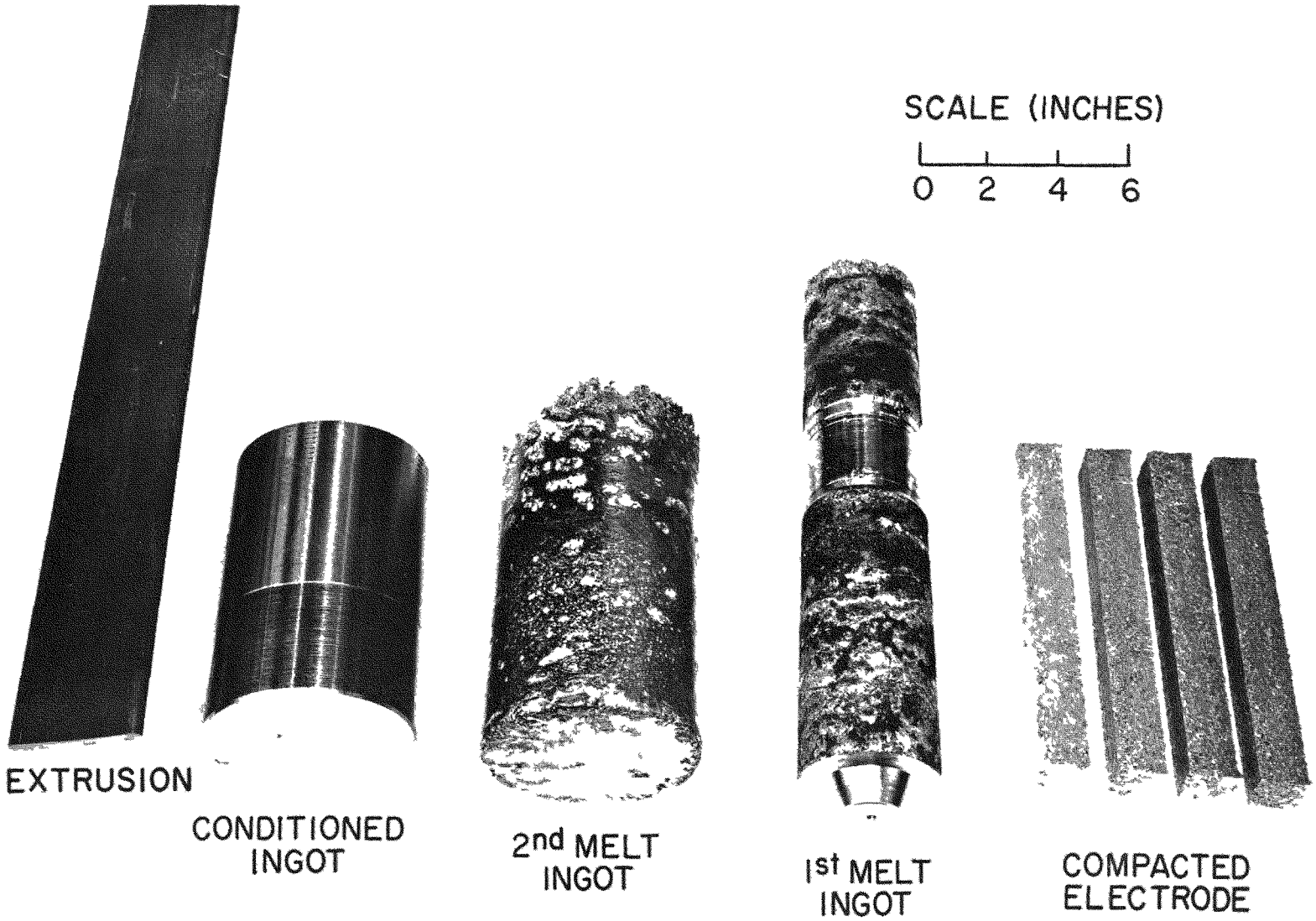

Figure 1. Zirconium Alloys - Processed Shapes

of which is shown in Figure 1. These ingots were remelted, under similar conditions, to produce the 6-in.-dia second melt ingots, each weighing approximately 40 lb. To remove surface defects, each of the second melt ingots was machined to a final diameter of 5-1/2 in.

After mechanical conditioning, the ingots were inspected by ultrasonic techniques. All of the ingots were sound except for minor shrink holes located within an inch to an inch and a quarter of the top of an ingot.

A complete chemical analysis, shown in Table IV, was performed on chips taken from the zirconium control ingot. Table V shows results of analysing the alloyed ingots for carbon, nitrogen, and the alloying elements. Complete chemical analyses were not made on the alloyed ingots because it was reasoned that the results obtained for the zirconium control ingot also applied to the alloys. Since no variables were introduced in either the sponge or the melting practice, this approach is justified.

TABLE IV

CHEMICAL ANALYSIS FOR ZIRCONIUM CONTROL INGOT

(Analysis in ppm)

Sn	Fe	Cr	Ni	Cu	W	N*	C	Al	B
<50	1560	40	19	<20	<20	29	<250	55	<0.3
Cd	Co	Hf	Pb	Mg	Mn	Mo	Si	Ti	V
<0.3	<10	<125	26	<10	29	<10	51	10	<10

* Kjeldahl method.

D. EXTRUDING

The conditioned ingots were extruded, bottom end forward, into bars of a 3-1/4-in. by 3/8-in. cross-section. For extruding, the ingots were induction-heated in open air to temperatures in the range 1850 to 1900°F. Short time heating cycles were employed as a means of retarding surface oxidation and oxygen diffusion. The data contained in Table VI represent upsetting and extruding pressures calculated from pressure measurements made on the ram of the extrusion press.

TABLE V

CHEMICAL ANALYSES FOR ALLOYED ZIRCONIUM INGOTS

(Analyses in wt %)

Alloy No.	Aluminum		Tin		Molybdenum		Carbon		Nitrogen*	
	Top	Bottom	Top	Bottom	Top	Bottom	Top	Bottom	Top	Bottom
2	1.58	1.63	-	-	-	-	<0.025	<0.025	0.0056	0.0032
3	1.45	1.44	1.53	1.51	-	-	<0.025	<0.025	0.0029	0.0028
4	1.44	1.40	2.91	3.03	-	-	<0.025	<0.025	0.0027	0.0025
5	1.51	1.46	-	-	1.37	1.38	<0.025	<0.025	0.0038	0.0035
6	1.40	1.38	1.59	1.55	1.33	1.37	<0.025	<0.025	0.0034	0.0057
7	3.05	3.07	-	-	-	-	<0.025	<0.025	0.0028	0.0031
8	3.00	2.99	1.46	1.59	-	-	<0.025	<0.025	0.0029	0.0032
9	3.19	3.00	2.85	3.00	-	-	<0.025	<0.025	0.0027	0.0028
10	3.12	3.05	1.56	1.65	1.39	1.31	<0.025	<0.025	0.0029	0.0055
11	2.15	2.20	-	-	-	-	<0.025	<0.025	0.0031	0.0029

TABLE VI

ZIRCONIUM ALLOY EXTRUSION PRESSURES

Alloy (wt %)	Billet Upsetting & Crushing Pressures (psi)	Extruding Pressures (psi)
Zirconium	49,600	29,200
Zr + 1.5 Al	96,000	48,000
Zr + 1.5 Al + 1.5 Sn	105,000	50,000
Zr + 1.5 Al + 3 Sn	115,000	62,000
Zr + 1.5 Al + 1.5 Mo	108,000	72,000
Zr + 1.5 Al + 1.5 Sn + 1.5 Mo	96,000	65,300
Zr + 3 Al	79,000	54,000
Zr + 3 Al + 1.5 Sn	92,600	61,800
Zr + 3 Al + 3 Sn	92,700	68,500
Zr + 3 Al + 1.5 Sn + 1.5 Mo	106,000	72,000
Zr + 2 Al	58,400	48,600

E. INSPECTION OF EXTRUSIONS

The extrusions were inspected for subsurface defects. For subsurface inspection, radiographs were taken through the 3/8-in. dimension of each extrusion. To confirm the existence of the few defects found near the back ends of the extrusions, sections for macroexaminations were taken from the front and back of each extrusion. Typical macroetched sections are shown in Figure 2. Approximately 1 ft at the back end of a 10-ft-long extrusion contained a defect similar to that shown in the top section of Figure 2. This portion was cropped from each extrusion prior to hot rolling.

The extrusion surfaces showed striations produced by the galling of the dies, but were free of other defects.

F. HOT ROLLING

In order to establish minimum rolling temperatures for the zirconium alloys, a preliminary study was made on strips cut from each extrusion. The strips, 6 in. by 1 in. by 3/8 in., were taken from the back end of each extrusion.

In the preliminary study, rolling was begun at relatively low temperatures where, as expected, severe edge cracking occurred. Other strips were rolled at increasing temperatures, until strips free of edge cracks were produced. This procedure established that unalloyed zirconium could be rolled at 1100°F, that the alloys containing 1.5% and 2% aluminum could be rolled at 1650°F, and that alloys containing 3% aluminum could be rolled at 1800°F. In no case could the 1.5% and 2% aluminum alloys be rolled free of edge cracks below 1450 to 1500°F. For the 3% aluminum alloys, this temperature range was 1650 to 1700°F. A preheating time of 15 minutes was found to be adequate for the 3/8-in.-thick extruded section. Two minute reheating cycles after each pass were found to be satisfactory.

As the hot rolling schedule for the zirconium alloys, presented in Table VII indicates, the rolling temperatures varied with the alloy content. More specifically, it was found that the rolling temperatures had to be increased with increasing aluminum content.

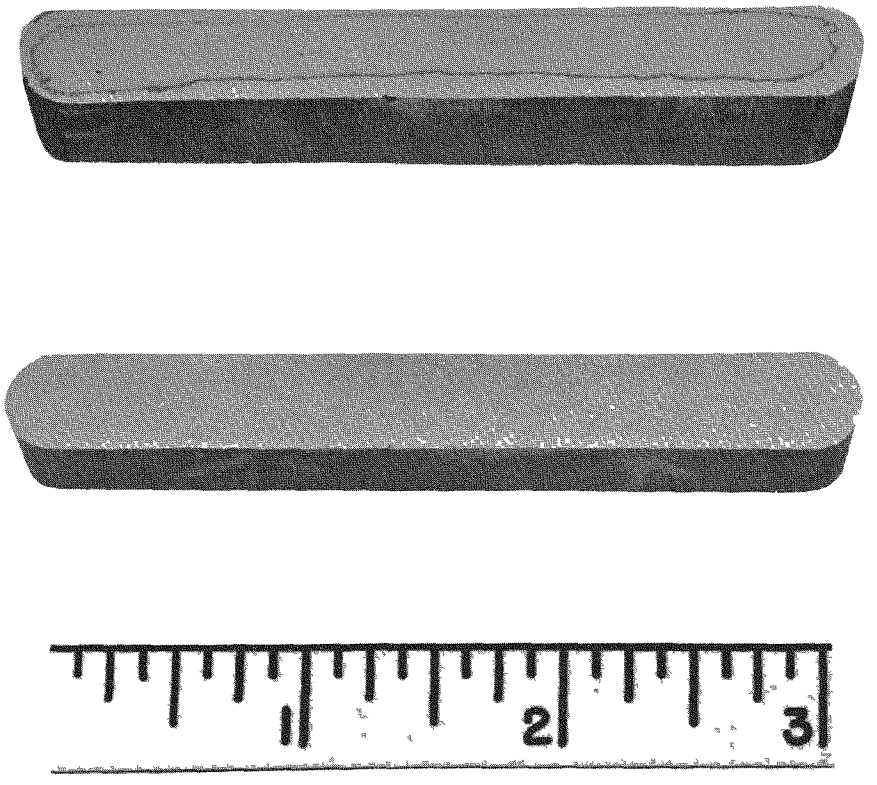

Fig. 2. Macroetched Sections From Extruded Zirconium Alloy Bar

TABLE VII

HOT ROLLING SCHEDULE FOR ZIRCONIUM ALLOY STRIP

Alloy (wt %)	Temperature (°F)	No. of Passes	Average Finish Thickness (in.)	Total Length (in.)
Zirconium	1100	5	0.125	118
Zr + 1.5 Al	1650	5	0.122	171
Zr + 1.5 Al + 1.5 Sn	1650	6	0.123	183
Zr + 1.5 Al + 3 Sn	1650	5	0.124	213
Zr + 1.5 Al + 1.5 Mo	1650	4	0.124	181
Zr + 1.5 Al + 1.5 Sn + 1.5 Mo	1650	4	0.125	213
Zr + 3 Al	1800	4	0.120	188
Zr + 3 Al + 1.5 Sn	1800	4	0.121	212
Zr + 3 Al + 3 Sn	1800	4	0.122	141
Zr + 3 Al + 1.5 Sn + 1.5 Mo	1800	4	0.125	164
Zr + 2 Al	1650	4	0.123	83

For conversion of the 3/8-in.-thick extrusions to 1/8-in.-thick strips, a billet length of 12 in. was selected because the final strip length, following the 3 to 1 reductions, would be an optimum for the pickling and vacuum annealing processes to follow.

The surface produced during the hot rolling operation was typical for zirconium heated and hot-worked in open air. The white zirconium oxide was apparent under a thin, hard, light brown surface scale. The light brown surface color has been attributed to the lubricant used during rolling.

G. CLEANING

In preliminary pickling studies, unsuccessful attempts were made to remove the oxide scale. It was found that acid pickling alone did not remove all of the scale and that very irregular surfaces, with localized areas of severe pitting, were produced. The pickling solutions used in these studies were composed of nitric and hydrofluoric acids, where the nitric acid was varied from 10 to 45% with the hydrofluoric acid content in the range 4 to 5%. Bath temperatures were maintained in the range 90 to 100°F.

Satisfactory cleaning was obtained by sandblasting the material prior to pickling. After the surfaces had been sandblasted free of scale, pickling in a bath composed of 45% nitric acid and 5% hydrofluoric acid, produced clean, uniform surfaces. About 0.002 to 0.003 in. of metal was removed after pickling for approximately 2 minutes, at 90 to 100°F.

H. VACUUM ANNEALING

Chemical analysis, performed on the sand blasted and pickled material, indicated hydrogen contents in the range of 50 to 100 ppm, as shown in Table VIII.

TABLE VIII

EFFECT OF PROCESSING STAGES ON THE HARDNESS AND HYDROGEN CONTENT

Alloy (wt %)	Hardness			Hydrogen Content (ppm)	
	Extruded	Hot Rolled	After Anneal	Hot Rolled Blasted & Pickled	After Anneal
Zirconium	82 R_B	90 R_B	85 R_B	46.7	15.9
Zr + 1.5 Al	21 R_C	28 R_C	22 R_C	59.0	11.7
Zr + 1.5 Al + 1.5 Sn	25	30	29	53.3	17.0
Zr + 1.5 Al + 3 Sn	26	28	28	69.4	11.9
Zr + 1.5 Al + 1.5 Mo	32	28	28	69.2	15.1
Zr + 1.5 Al + 1.5 Sn + 1.5 Mo	33	28	31	63.6	15.3
Zr + 3 Al	32	32	29	91.8	11.3
Zr + 3 Al + 1.5 Sn	32	31	30	73.7	10.4
Zr + 3 Al + 3 Sn	33	30	29	80.8	14.0
Zr + 3 Al + 1.5 Sn + 1.5 Mo	38	40	30	59.0	12.3
Zr + 2 Al	29	27	27	84.7	13.5

Because hydrogen reduces the room temperature ductility of zirconium[5] and zirconium alloys, a vacuum-annealing operation was performed to remove most of this interstitial. A second objective of vacuum annealing was to produce a uniform microstructure, free of the effects of prior work. The effects of this operation on the hydrogen content, as well as the effects of rolling and annealing on the hardness of the alloys, are shown in Table VIII.

Initial tests were performed to establish the furnace characteristics under operating conditions. The results of these tests indicated that a pressure of approximately 0.04 microns could be maintained with the furnace operating at 1450°F. It was also found that at this temperature, a uniform temperature zone existed over a 4- to 5-ft length, which was adequate for the 36-in.-long strips.

Following a thorough degreasing in trichloroethylene, the strips were suspended vertically in the retort of the vacuum furnace. The strips were annealed at a temperature of 1450°F for 24 hr. The pressure, at the end of 24 hr, was less than 0.2 microns of mercury. A typical annealing-cycle log is shown in Table IX.

TABLE IX

LOG OF VACUUM ANNEALING CYCLE

Date	Time	Temperature	Pressure (microns)	Remarks
1 July 1958	3:00 p.m.	-	-	Furnace loaded
1 July 1958	4:30 p.m.	500°F	-	Pressure too high to read on vacuum gauge
2 July 1958	10:00 a.m.	1450°F	30	Load reached temperature, material outgassing
3 July 1958	4:00 p.m.	1450°F	0.18	Furnace turned off
3 July 1958	10:30 p.m.	1050°F	-	Diffusion pump turned off, mechanical roughing pump left running
7 July 1958	8:00 a.m.	150°F	-	Furnace unloaded

After annealing, the surfaces of the strips appeared to be the same as the pickled surfaces. There was no discoloration or other traces of oxidation. It was also noticed that during the annealing operation the strips had straightened under their own weight.

III. TEST RESULTS AND DISCUSSION

A. SODIUM COMPATIBILITY TESTING

An important factor to be considered in the evaluation of a cladding material is its corrosion resistance in the operating environment. Therefore early consideration was given to the initiation of sodium compatibility studies.

From each of the extruded bars, 20 test specimens, 1 by 1/2 by 1/4 in. were machined. All surfaces of the specimens were machined to a specified finish of 63 micro-in. RMS. Prior to exposure, each specimen was carefully cleaned and weighed to the nearest 0.1 milligram. Dimensions were measured to the nearest 0.001 in.

The specimens were exposed to sodium at 1000°F in a system where the oxygen level was maintained at 10 ppm by a cold trap operated at 290°F. Sodium flow was maintained by natural convection. The corrosion specimens were suspended in sodium for predetermined periods of time, after which they were washed, dried, and reweighed. Following exposure, the specimens exhibited a thin, tightly adherent, blue-black film.

The weight change data tabulated in Table X represent the averages for duplicate specimens at each condition. For comparison, the data for unalloyed zirconium under the same exposure conditions are included. Figure 3 is a graphical representation of the total weight-gain versus the log of time, where data for the Zr + 1.5 Al + 1.5 Mo, the Zr + 3 Al + 3 Sn alloys, and for unalloyed zirconium are shown. These two alloys represent the extremes of the complete series.

The data show that the specimens gained weight as a function of time. The discontinuity of data can be attributed to interrupted tests after 300 hr and again after 1000 hr. Despite these interruptions, the general trend seems well enough defined to conclude that the weight-gain rates for the zirconium alloys are approximately equal to the rate for unalloyed zirconium. In addition, a comparison of the weight-gain data for the various alloys indicates that those alloys which contain tin consistently show lower weight-gains.

TABLE X

CORROSION OF ZIRCONIUM AND ZIRCONIUM ALLOYS IN 1000°F SODIUM

Alloy (wt %)	Average Weight Gain (Mg/cm^2)						
	75 hr	163 hr	303 hr	500 hr	1000 hr	1500 hr	2500 hr
Zr	0.14	0.23	0.33	0.30	0.55	0.50	0.56
Zr + 1.5 Al	0.16	0.26	0.37	-	-	-	-
Zr + 1.5 Al + 1.5 Sn	0.14	0.24	0.36	-	-	-	-
Zr + 1.5 Al + 3 Sn	0.15	0.21	0.27	0.27	0.49	0.38	0.41
Zr + 1.5 Al + 1.5 Mo	0.22	0.35	0.44	0.46	0.73	0.61	0.59
Zr + 1.5 Al + 1.5 Sn + 1.5 Mo	0.18	0.33	0.40	-	-	-	-
Zr + 3 Al	0.18	0.25	0.31	-	-	-	-
Zr + 3 Al + 1.5 Sn	0.17	0.25	0.29	0.30	0.45	0.39	0.39
Zr + 3 Al + 3 Sn	0.17	0.22	0.27	0.26	0.45	0.35	0.35
Zr + 3 Al + 1.5 Sn 1.5 Mo	0.23	0.31	0.36	0.35	0.56	0.43	0.52
Zr + 2 Al	0.17	0.26	0.39	-	-	-	-

B. ROOM AND ELEVATED TEMPERATURE TENSILE PROPERTIES

The zirconium and zirconium alloy coupons used in this series of tests were prepared from extruded, rolled, and vacuum-annealed strips. To eliminate any possible effects of surface contamination, the coupon blanks taken from the strips were surface-ground to a depth of 0.010 to 0.015 in. on each side. After surface grinding, standard 2-in. gage length tensile coupons were milled from the blanks. Typical test specimens are shown in Figure 4. Prior to testing, the reduced section of each test coupon was hand-polished longitudinally to eliminate possible stress raisers. For the elevated temperature tests, reenforcing tabs were welded on each grip end. In welding the tabs, chill blocks prevented heat effects in the test section.

The tensile tests were conducted in a 60,000-lb hydraulic testing machine with attached strain-pacer and recorder. A strain rate of approximately 0.00075 per min was used for all of the tensile tests. For room temperature tests, a

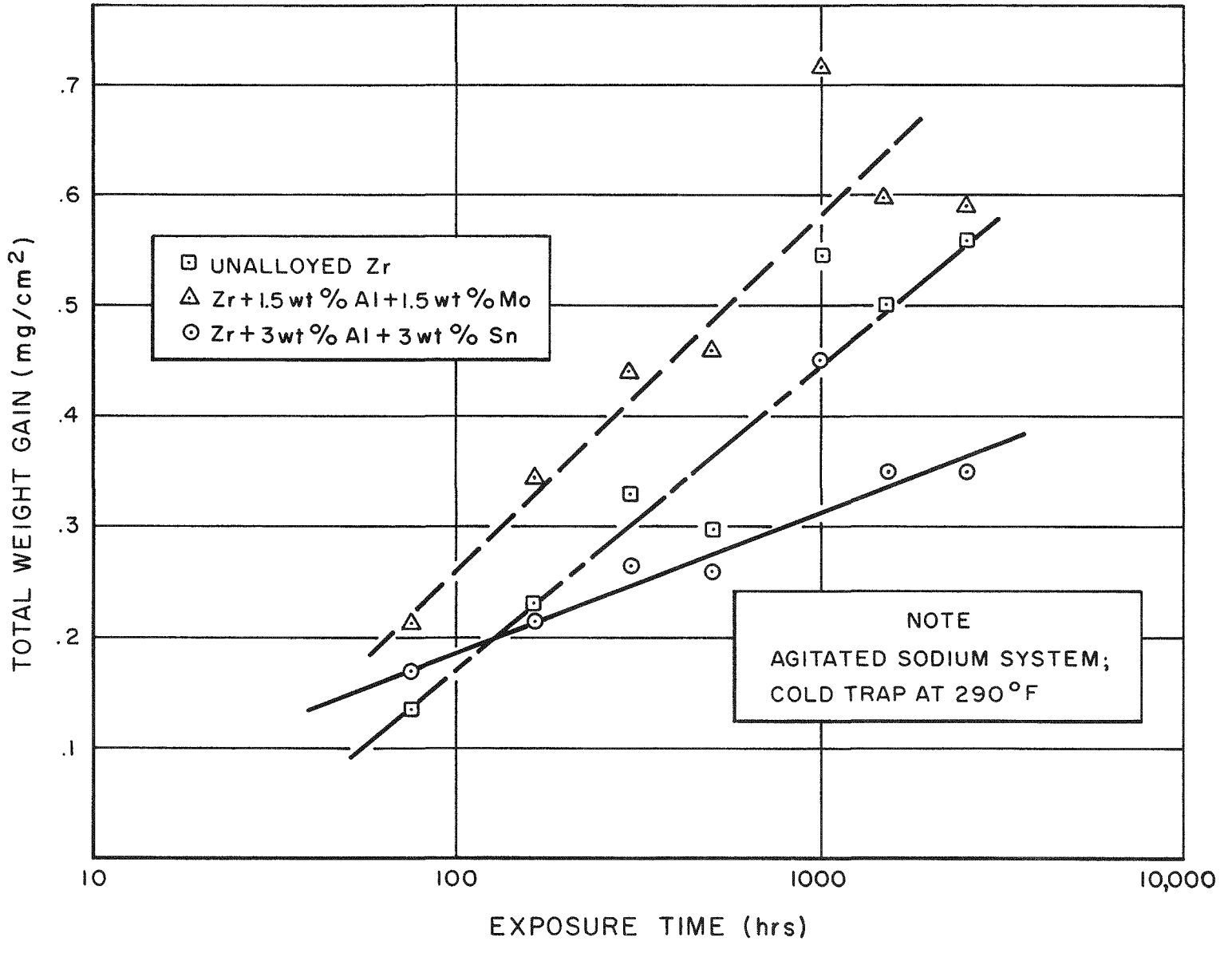

Figure 3. Corrosion of Zirconium Base Alloys in Sodium at 1000°F

snap-on extensometer was used. A separable, variable-reluctance extensometer was used for the elevated temperature tests. Both extensometers were designed to accommodate 2-in. gage length sections.

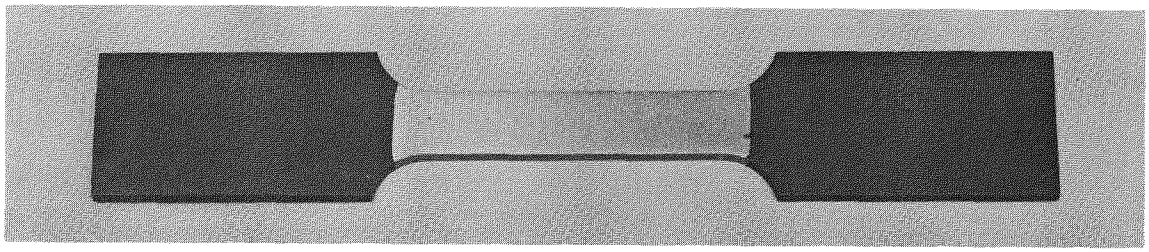

ROOM TEMPERATURE SPECIMEN

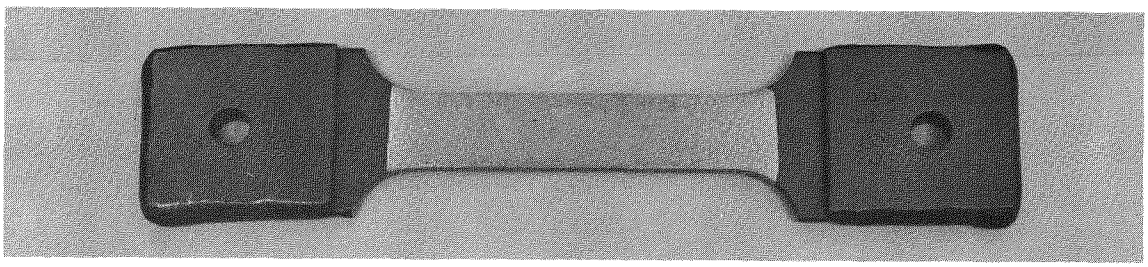

ELEVATED TEMPERATURE SPECIMEN

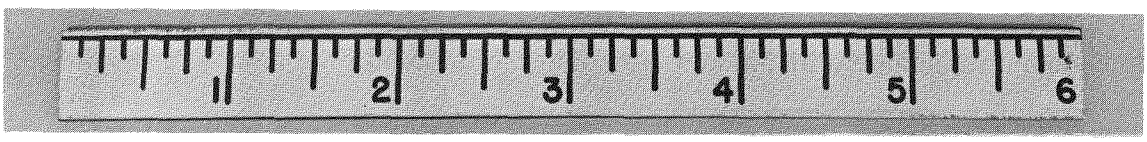

Figure 4. Typical Tensile Specimens

All of the elevated temperature tests were conducted in helium-filled chambers. Temperatures were controlled to ± 3°F by a thermocouple attached to the midpoint of the tensile coupon. The test coupons were allowed to soak at the test temperature for at least one hour before loads were applied.

In addition to the zirconium alloys, other sheet materials investigated in this series of tests included type 304 stainless steel and Zircaloy 2. The stainless steel sheet was procured on Material Specification Mil-S-854, Condition A (annealed); and the Zircaloy 2 strip was reactor grade.

All tests were conducted in duplicate, hence the data included in Tables XI, XII, and XIII represent the average of two determinations. With the exception of the values for percent elongation, all of the tensile data reported were taken from autographic recordings.

TABLE XI

TENSILE PROPERTIES AT ROOM TEMPERATURE

Alloy (wt %)	0.2% Offset Yield Strength (10^3 psi)	Ultimate Tensile Strength (10^3 psi)	Elongation (% in 2 in.)	Modulus of Elasticity (10^6 psi)
Zr	35.5	62.0	18	17.9
Zr + 1.5 Al	82.9	99.0	17.5	16.5
Zr + 1.5 Al + 1.5 Sn	87.5	101.4	13	16.1
Zr + 1.5 Al + 3 Sn	103.0	114.5	13	14.7
Zr + 1.5 Al + 1.5 Mo	115.5	121.6	8.5	14.4
Zr + 1.5 Al + 1.5 Sn + 1.5 Mo	118.0	127.3	10.0	13.6
Zr + 3 Al	115.8	129.4	11.5	15.2
Zr + 3 Al + 1.5 Sn	118.3	133.4	11.0	14.9
Zr + 3 Al + 3 Sn	122.3	136.8	3.0	17.0
Zr + 3 Al + 1.5 Sn 1.5 Mo	114.6	132.5	9.5	17.4
Zr + 2 Al	90.2	107.2	13.5	15.4
Zircaloy 2	40.5	70.5	21	16.7
Stainless Steel, Type 304	37.2	85.2	44	28.9

The effect of increasing amounts of the alloying elements is quite apparent. The ultimate and yield strengths of the alloys are substantially greater than those of unalloyed zirconium. As expected, the increases in strength are accompanied by decreases in ductility. A graphic representation of the strengthening effect of aluminum on the yield strength of zirconium is shown in Figure 5. From these data, it can be seen that aluminum additions markedly strengthen zirconium at both room and elevated temperatures. Similar results on the strengthening effect of aluminum in zirconium have been described.[1,2,3,4]

TABLE XII

SHORT TIME TENSILE PROPERTIES AT 1050°F

Alloy (wt %)	0.2% Offset Yield Strength (10^3 psi)	Ultimate Tensile Strength (10^3 psi)	Elongation (% in 2 in.)	Modulus of Elasticity (10^6 psi)
Zr	5.7	13.5	66	10.5
Zr + 1.5 Al	34.0	47.3	31	9.6
Zr + 1.5 Al + 1.5 Sn	40.4	54.5	22.5	9.3
Zr + 1.5 Al + 3 Sn	42.0	60.8	25.5	8.3
Zr + 1.5 Al + 1.5 Mo	43.0	54.0	27	8.1
Zr + 1.5 Al + 1.5 Sn + 1.5 Mo	45.9	63.5	31	11.3
Zr + 3 Al	49.1	73.3	23	11.6
Zr + 3 Al + 1.5 Sn	48.1	77.1	25.5	14.5
Zr + 3 Al + 3 Sn	52.1	78.7	17.5	9.8
Zr + 3 Al + 1.5 Sn + 1.5 Mo	48.5	70.1	30.0	10.2
Zr + 2 Al	42.9	59.1	24.3	8.4
Zircaloy 2	10.7	19.5	64.8	8.9
Stainless Steel, Type 304	24.5	56.7	31.5	17.2

The superior tensile properties of these zirconium alloys are further demonstrated by comparing their tensile properties with those of Zircaloy 2 and of type 304 stainless steel. The data in Tables XI, XII, and XIII show that the tensile properties of the alloys exceed those of Zircaloy 2 and of type 304 stainless steel at both room and elevated temperatures.

Increasing the temperature from 80 to 1050°F produces the expected loss in strength and increase in elongation. The percent loss in strength for the alloys as a group is substantially less than the loss for unalloyed zirconium. The alloys show a 39% decrease in tensile strength between room temperature and 1050°F. The tensile strength of unalloyed zirconium decreases 77% over the same range, and type-304 stainless steel shows a 40% decrease. A further increase in temperature to 1200°F produced a continued loss in strength which is much more pronounced for the zirconium alloys than for type-304 stainless steel.

TABLE XIII

SHORT TIME TENSILE PROPERTIES AT 1200°F

Alloy (wt %)	0.2% Offset Yield Strength (10^3 psi)	Ultimate Tensile Strength (10^3 psi)	Elongation (% in 2 in.)	Modulus of Elasticity (10^6 psi)
Zr	3.1	7.4	134.0	8.5
Zr + 1.5 Al	25.2	36.6	39.5	5.7
Zr + 1.5 Al + 1.5 Sn	30.5	43.4	26.7	6.1
Zr + 1.5 Al + 3 Sn	34.0	48.2	32.0	6.2
Zr + 1.5 Al + 1.5 Mo	26.9	40.0	38.7	7.4
Zr + 1.5 Al + 1.5 Sn 1.5 Mo	30.6	44.7	41.7	6.5
Zr + 3 Al	36.5	57.9	32.5	6.3
Zr + 3 Al + 1.5 Sn	33.1	56.9	24.0	5.1
Zr + 3 Al + 3 Sn	39.0	67.1	15.0	7.4
Zr + 3 Al + 1.5 Sn + 1.5 Mo	31.8	47.3	33.5	6.8
Zr + 2 Al	31.2	45.3	43	7.7
Zircaloy 2	6.4	13.2	80	4.7
Stainless Steel, Type 304	23.4	48.1	32	12.4

C. CREEP TESTING

The procedure used in preparing the test coupons for this series of tests was similar to that described in the section on tensile properties. Specimens of the type shown in Figure 4 were used for all creep tests.

All of the creep tests were performed in constant-load creep machines, where a lever-arm loading system with a 20:1 mechanical advantage is used. The specimens were heated to 1050 ± 3°F in argon-filled chambers where the argon, maintained at a constant pressure of 5 psig, was passed through a combination NaK bubbler and scrubber prior to its introduction into the chamber. Before the load was applied, the thermocoupled specimen was allowed to soak at the test temperature for approximately one hour. Elongation readings were taken regularly over a period of 200 to 600 hr.

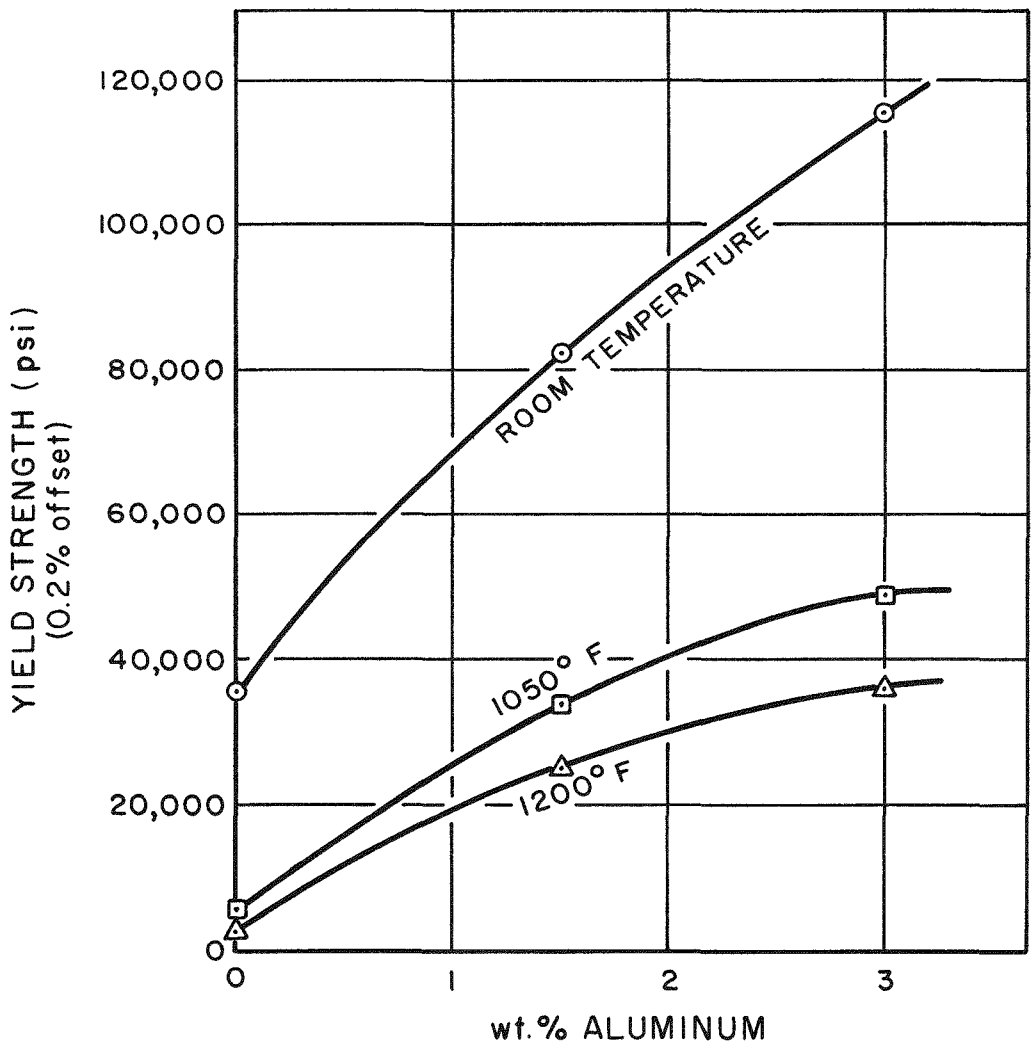

Figure 5. Effect of Increasing Aluminum on the Yield Strength of Zirconium

The data included in Table XIV were determined for all of the alloys at a constant stress level of 25,000 psi, to screen the alloys on the basis of their

TABLE XIV

MINIMUM CREEP RATES FOR ZIRCONIUM ALLOYS AT 1050°F

Alloy (wt %)	Stress (10^3 psi)	Minimum Creep Rate (% per hr)
Zr + 1.5 Al	25	2×10^{-1}
	25	1.5×10^{-1}
Zr + 1.5 Al + 1.5 Sn	25	1.5×10^{-2}
Zr + 1.5 Al + 3 Sn	25	2.3×10^{-2}
Zr + 1.5 Al + 1.5 Mo	25	1.3×10^{-2}
Zr + 1.5 Al + 1.5 Sn + 1.5 Mo	7.5	5×10^{-4}
	12.5	1.8×10^{-3}
	17.5	3.8×10^{-3}
	25	1.3×10^{-2}
	25	1.7×10^{-2}
Zr + 3 Al	25	6.5×10^{-2}
	25	1.6×10^{-2}
Zr + 3 Al + 1.5 Sn	25	2.5×10^{-2}
	25	2.1×10^{-2}
Zr + 3 Al + 3 Sn	25	3.2×10^{-2}
	25	2.7×10^{-2}
Zr + 3 Al + 1.5 Sn + 1.5 Mo	5	9×10^{-4}
	12.5	2.1×10^{-3}
	25	7×10^{-3}
	30	1×10^{-2}
	35	5×10^{-2}
Zr + 2 Al	25	6×10^{-2}
Stainless Steel, Type 304	25	2×10^{-3}
	35	5×10^{-3}

creep strength. Further testing was then performed on only the more promising alloys. The unalloyed zirconium control was not included in this evaluation, since the 25,000-psi stress level is above its ultimate tensile strength at 1050°F.

The creep resistance for an alloy is reported as a minimum creep rate in % per hour. To arrive at the minimum creep rate, it was assumed that all of the elongation which occurred during the secondary stage took place in the 2-in. reduced section of the specimen. The use of this method for determining minimum creep rate was necessary, since the furnace and atmosphere chambers of the creep machines were not equipped with observation ports.

The effect of molybdenum on the minimum creep rates for two of the alloys is illustrated graphically in Figure 6. For the zirconium + 1.5% aluminum binary alloy, the addition of 1.5% molybdenum decreases the creep rate by a factor of 10. A similar addition to the ternary alloy, zirconium + 3% aluminum + 1.5% tin, produced a three-fold reduction in its creep rate.

Further indication of the effectiveness of molybdenum in retarding the creep rate of zirconium alloyed with the alpha-stabilizing elements -- aluminum and tin -- is demonstrated by comparing the creep rates for three of the alloys:

1) Zirconium + 1.5% aluminum

2) Zirconium + 1.5% aluminum + 1.5% molybdenum

3) Zirconium + 3% aluminum + 1.5% tin

The comparison shows that the addition of 1.5% molybdenum to the basic zirconium + 1.5% aluminum alloy has an effect equivalent to the addition of both 1.5% aluminum and 1.5% tin to the basic alloy.

D. THERMAL CONDUCTIVITY

Thermal conductivity values through the temperature region of 752 to 1157°F were determined for a selected group of the zirconium alloys and for type 304 stainless steel. The zirconium alloy wafers used for thermal conductivity measurements were machined from the unused portions of the extrusion billets. The stainless steel specimens were machined from bar stock which met the requirements of Material Specification QQ-S-763.

To measure the thermal conductivity, a radial heat flow method was employed. The values which are tabulated in Table XV represent the averages of at least three measurements for each alloy at each temperature. The graph shown in Figure 7 was prepared following conversion of the data in Table XV. In this

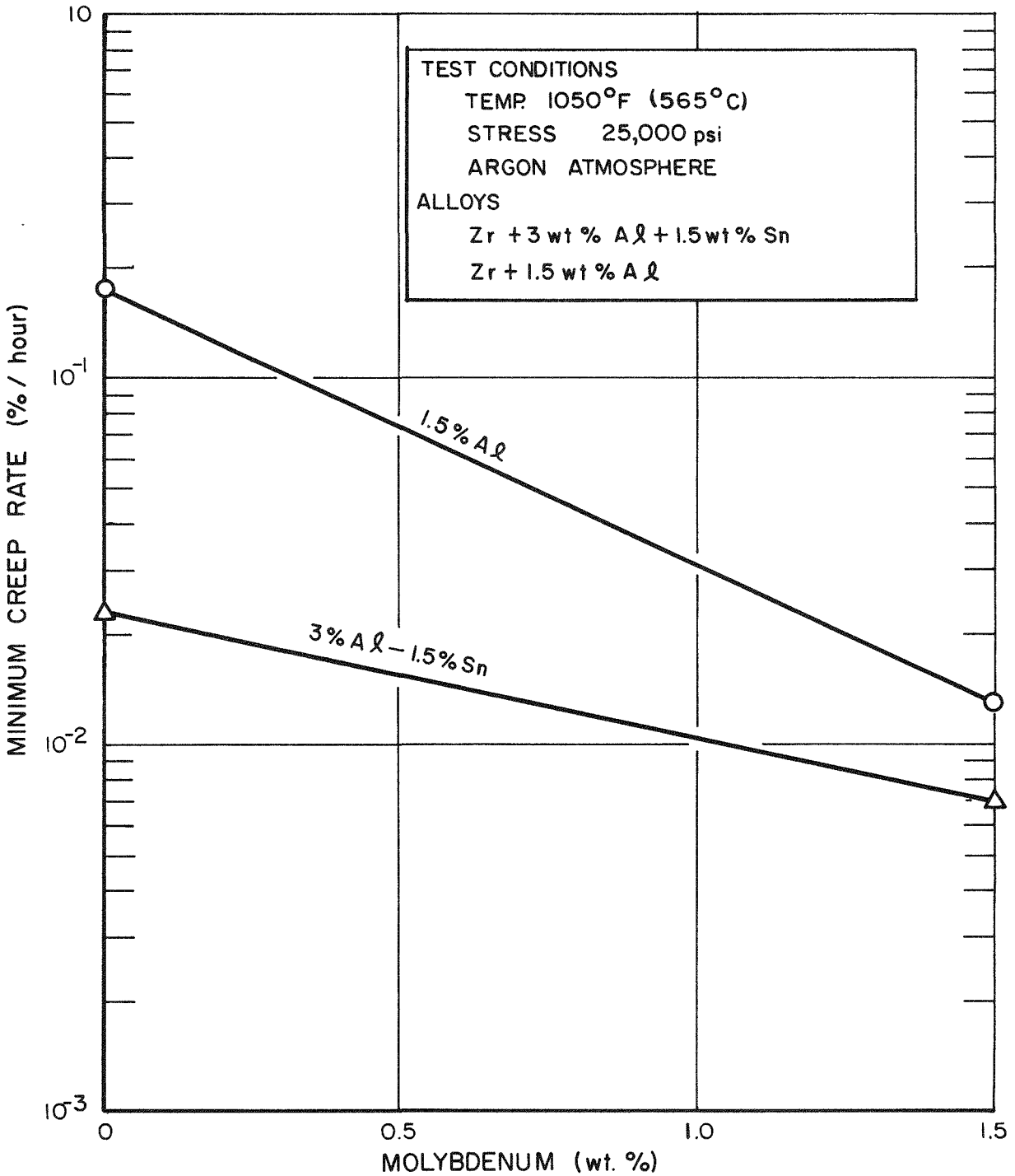

Figure 6. Effect of Molybdenum on the Minimum Creep Rates for Two Zirconium Base Alloys

TABLE XV

THERMAL CONDUCTIVITY FOR A SELECTED GROUP OF ZIRCONIUM BASE ALLOYS AND STAINLESS STEEL

Alloy	Temperature (°F)*	Thermal Conductivity (Btu/hr-ft-°F)*	Alloy	Temperature (°F)*	Thermal Conductivity (Btu/hr-ft-°F)*
Type-304 Stainless steel	887	12.3	Zr + 3 Al + 1.5 Sn	793	7.2
	961	12.5		872	7.4
	1027	12.5		1017	7.9
	1090	13.1		1108	8.3
Zr +1.5 Al + 3 Sn	761	7.6	Zr + 3 Al + 3 Sn	851	8.1
	829	8.3		919	8.3
	896	8.7		966	8.5
	1013	9.0		1026	8.7
	1116	9.6		1105	9.2
Zr + 1.5 Al + 1.5 Sn + 1.5 Mo	885	9.6	Zr + 2 Al	914	9.5
	910	9.7		995	10.0
	995	9.9		1074	10.5
	1103	10.7		1159	10.6

* Converted from metric units. Also corrected with Type-304 stainless steel standard.

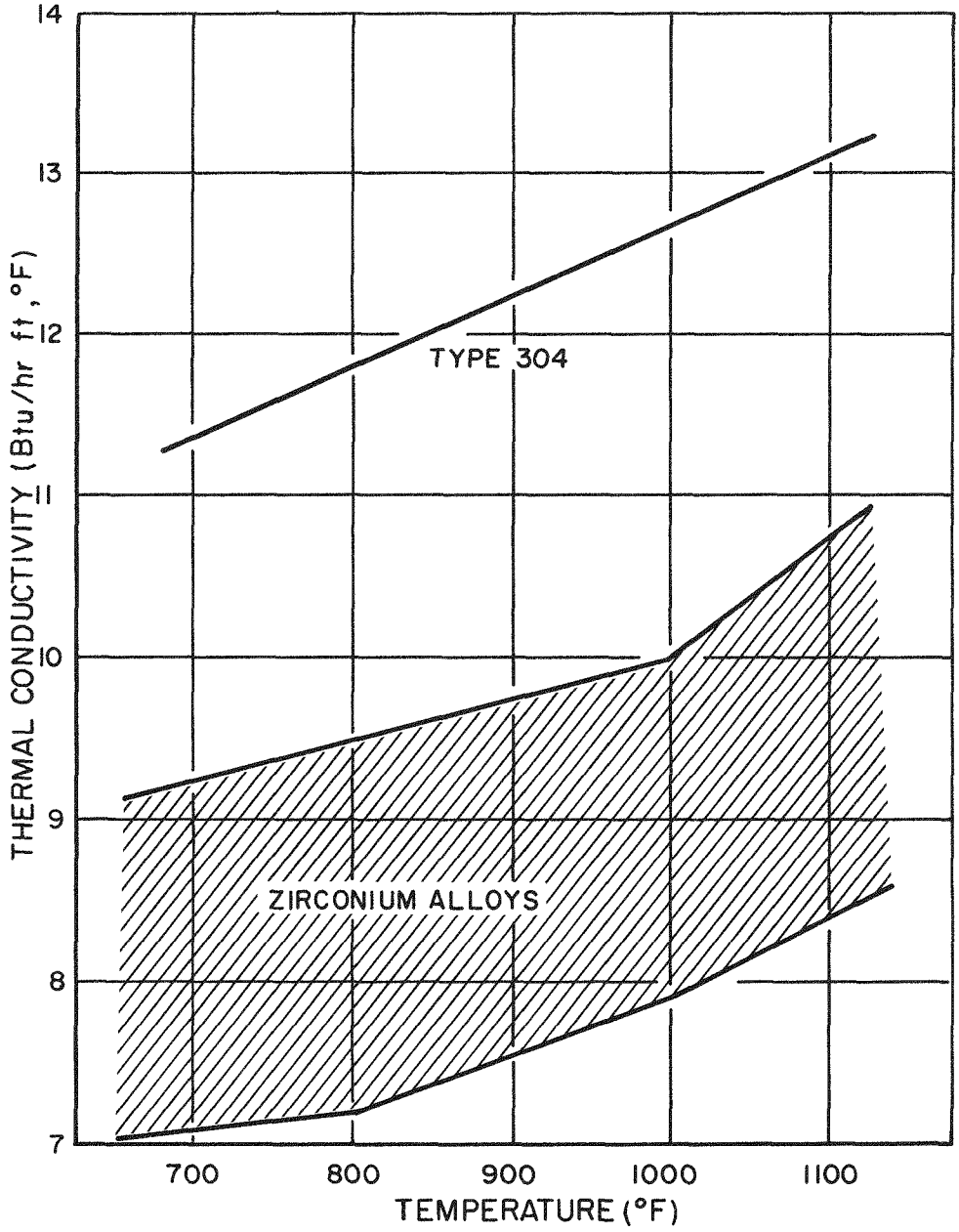

Figure 7. Thermal Conductivity of Zirconium Alloys and Stainless Steel

figure, the data for the alloys are presented as a band, the extremes of which represent the two alloys having the highest and the lowest thermal conductivity. Figure 7 shows that the thermal conductivity of the zirconium alloys averages 65 to 75% of the thermal conductivity for stainless steel over the temperature range investigated.

E. WELDING

The welding characteristics of a selected group of the zirconium alloys and the effects of welding on the tensile properties of these alloys were investigated on a preliminary basis. These studies were performed on vacuum-annealed sections of 3 by 3-1/4 by 1/8 in. After butt-welding, a total of eight coupons per alloy was taken for bend and tensile specimens. The axis of the weld was perpendicular to the longitudinal axes of the test specimens. Welding conditions are given in Table XVI.

TABLE XVI

WELDING CONDITIONS FOR ZIRCONIUM ALLOYS

Current	223 to 224 Amperes, d-c Straight Polarity
Arc Voltage	9 volts
Torch Speed	9 in. per min
Cover Gas	Argon, at 20 cfh
Back-up Gas	Helium, at 20 cfh

The integrity of the welds was evaluated by radiographic inspection and by bend-testing. Sound welds, free of porosity, were indicated by the X-ray examinations. Guided-bend tests were performed in accordance with the ASME Code for Unfired Pressure Vessels.

The bend test specimens, 6-in. by 1/2-in. by 0.100 in., were hand polished to remove stress raisers. Prior to the surface grinding, strips were divided into two groups, one of which was vacuum-annealed at 1450°F for 24 hr. Both root- and face-bends around a mandrel of 8T radius were made in a universal

testing machine. The bends were made at room temperature and at very slow loading rates.

All welded strips passed the bend test through 180° around an 8T radius. In these tests no difference was observed between root- and face-bends on both as-welded and vacuum-annealed test specimens. It was noted that all of the alloys exhibited a high degree of springback from the 180° bend-test position. For the lower alloys, the springback ranged from 45 to 60°. The higher alloys containing 3% Al + Sn experienced springback in the range of 60 to 78°. Typical examples of bend-test specimens are shown in Figure 8.

For the tensile tests, 2-in. gage length coupons were taken from the welded sections. To evaluate the effect of annealing, half of the coupons were vacuum-annealed at 1450°F for 24 hr. The results of the room temperature tensile tests are shown in Table XVII. All values represent an average of two tests. Tensile testing conditions and equipment have been previously described. A comparison of these data for the welded material with those in Table XI for the vacuum-annealed material at room temperature indicates that welding has only a slight effect on the room temperature tensile strength of the zirconium alloys investigated. However, the effect of welding on the ductility is more pronounced. In almost all instances, the elongation of the as-welded material is less than that for the original material. Vacuum-annealing after welding produced an improvement in elongation for only two of the alloys. It is apparent that further investigation of annealing effects on welds is necessary.

F. MICROSTRUCTURE

Metallographic studies were made at various stages in the processing and fabrication of the zirconium alloys.

The series of photomicrographs contained in Figure 9 show microstructures which were found to be typical for the Al-Zr binary alloys and for the Al-Sn-Zr ternary alloys at the processing stages indicated. It is apparent that the difference between the extruded structure and the rolled structure is a matter of grain size. This difference would be expected, considering that the extruding and rolling temperatures, as well as the cooling rates, were similar. The effect of the 1450°F anneal followed by air cooling is more pronounced. A two-phase

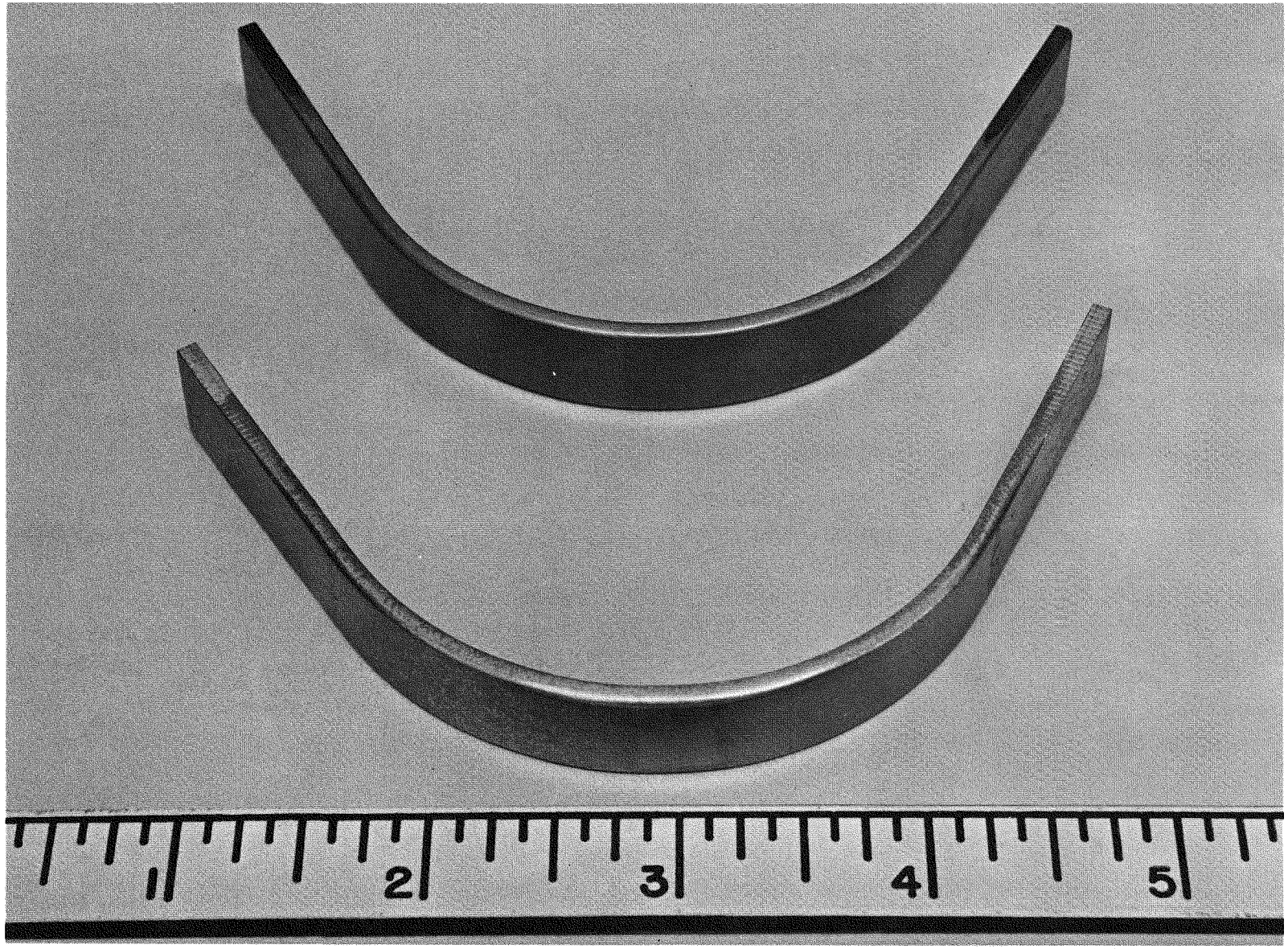

Figure 8. Bend Test Specimens

TABLE XVII

TENSILE PROPERTIES OF WELDED ZIRCONIUM ALLOYS

Alloy (wt %)	0.2% Offset Yield Strength (10^3 psi)	Ultimate Tensile Strength (10^3 psi)	Elongation (% in 2 in.)
Zr + 1.5 Al + 1.5 Sn	91.0	110.8	8.5
Zr + 1.5 Al + 1.5 Sn, Annealed	92.6	108.9	10.2
Zr + 1.5 Al + 3 Sn	101.7	117.6	9.7
Zr + 1.5 Al + 3 Sn Annealed	104.0	117.0	8.4
Zr + 1.5 Al + 1.5 Mo	109.4	118.9	7.5
Zr + 1.5 Al + 1.5 Mo, Annealed	114.3	121.2	8.0
Zr + 3 Al + 1.5 Sn	122.2	134.2	13.5
Zr + 3 Al + 1.5 Sn, Annealed	122.7	132.4	12.5
Zr + 3 Al + 3 Sn	124.0	137.1	6.5
Zr + 3 Al + 3 Sn, Annealed	122.8	132.2	2

NOTE: All fractures occurred in parent metal.

structure, composed of alpha zirconium and an aluminum-zirconium intermetallic compound (possibly Zr_3Al), is evident. For the vacuum-annealed photomicrograph in Figure 9, higher magnification showed the finely precipitated second phase. This precipitate was not evident in either the extruded or rolled structures when examined at 500 x.

The photomicrographs in Figure 10 show the microstructures produced at various processing stages for one of the Al-Sn-Mo-Zr quaternary alloys. The addition of molybdenum, a beta stabilizer, produces microstructures which are predominantly two-phase. Identification of the various phases was not made.

G. ABSORPTION CROSS-SECTION

It is zirconium's low absorption cross-section for thermal neutrons which makes the material so attractive for nuclear reactor applications. In order to retain this property, only elements having relatively low absorption cross-sections were considered for alloying purposes.

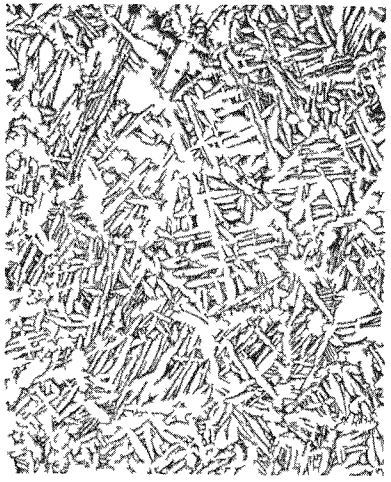

AS EXTRUDED
100 x

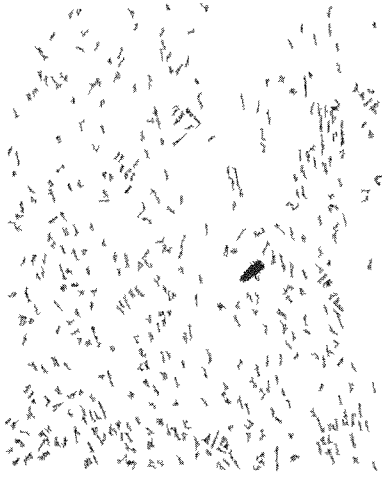

AS ROLLED
100 x

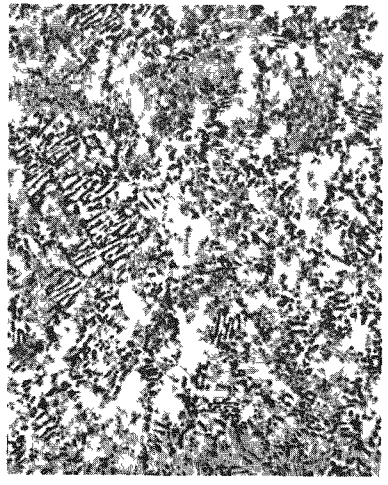

VACUUM ANNEALED
500 x

LONGITUDINAL ETCHANT 5% $AgNO_3$ + 2% HF

Figure 9. Microstructures of Zirconium Alloy - Zr + 3 wt % Al

AS EXTRUDED
500 x

AS ROLLED
500 x

VACUUM ANNEALED
500 x

LONGITUDINAL ETCHANT 5% $AgNO_3$ - 2% HF

Figure 10. Microstructures of Zirconium Alloy - Zr + 1.5 wt % Al + 1.5 wt % Sn + 1.5 wt % Mo

The absorption cross-sections for unalloyed zirconium, for the most highly alloyed zirconium alloy, and for Type-304 stainless steel are presented in Table XVIII. These values show that the low absorption cross-section for unalloyed zirconium has not been seriously affected by the addition of 3% aluminum, 1.5% tin and 1.5% molybdenum.

TABLE XVIII

MACROSCOPIC ABSORPTION CROSS-SECTIONS

Material	cm^{-1}
Zirconium	0.0078
Zr + 3 Al + 1.5 Sn + 1.5 Mo Alloy	0.010
Stainless Steel, Type 304	0.26

A comparison between the value for unalloyed zirconium with that for stainless steel clearly demonstrates the superiority of the nonferrous material in minimizing parasitic neutron absorption.

The values for the alloys in Table XVIII were obtained by relatively simple calculations. For any alloy, the macroscopic cross-section is given by:

$$\Sigma_{alloy} = N_1\sigma_1 + N_2\sigma_2 + \ldots N_n\sigma_n$$

$$= \frac{N_a}{100}\left[\left(\frac{W_1\rho}{A_1}\right)\sigma_1 + \left(\frac{W_2\rho}{A_2}\right)\sigma_2 + \ldots \left(\frac{W_n\rho}{A_n}\right)\sigma_n\right] ,$$

where

Σ = macroscopic cross-section,
W = weight % of the element,
ρ = density of the alloy,
N_a = Avogradro's number,
A = atomic weight of the element, and
σ = microscopic absorption cross-section for the element, 10^{-24} cm^2/atom.

IV. CONCLUSIONS

A. For the zirconium alloys studied in this program, it can be concluded that:

1) They can be successfully hot-worked by standard fabricating techniques.

2) Their corrosion resistance is, with slight variation, equal to that for unalloyed zirconium after 2500-hr exposure in sodium at 1000°F.

3) Their tensile strength, at room and at elevated temperatures, is greater than that for unalloyed zirconium, and comparable to that of type-304 stainless steel.

4) Their average thermal conductivity, equal to 75% of that of stainless steel, is considered to be adequate for nuclear reactor service.

5) Their creep resistance, although less than that for type-304 stainless steel, is acceptable for reactor use.

6) The alloys can be welded by standard shielded tungsten arc techniques with no serious loss in ductility or strength.

7) Their neutron absorption characteristics vary only slightly from that of unalloyed zirconium.

B. On the basis of these conclusions, an alloy containing 1.5 wt % Al + 1.0 wt % Sn + 1.0 wt % Mo has been selected for investigation on a larger scale. It has been concluded that an alloy of the selected analysis will demonstrate a good combination of properties with respect to strength and creep resistance at elevated temperatures, corrosion resistance to liquid sodium, and hot and cold fabricability.

In such an alloy, the element aluminum would contribute to the strength characteristics, tin would impart corrosion-inhibiting characteristics, and molybdenum would provide improved resistance to creep at moderately high temperatures.

V. FUTURE WORK

A. Further study of the high-strength zirconium alloys investigated should include their:

1) Cold-forming characteristics.

2) Welding and heat-treating response.

3) Germinative grain-growth characteristics.

4) Resistance to fatigue.

B. Material of the selected composition will be prepared for a fabrication effort to include the production of such mill products as tubing, sheet and bar stock.

C. Mill products obtained in the fabrication effort will be fabricated into fuel elements and subsequently placed in the Sodium Reactor Experiment core for evaluation of their in-reactor characteristics.

REFERENCES

1. W. Chubb, "Progress in the Development of Creep-Resistant Zirconium Alloys," Transactions of American Society for Metals 48, 1956, p.804.
2. R.J. Van Thyne and D.J. Mc Pherson, "Elevated Temperature Strength of Selected Zirconium-Base Alloys," Transactions of American Society for Metals 48, 1956, p.795.
3. J.H. Keeler, "Development of Zirconium-Base Alloys," SO-2526, November, 1956.
4. B. Lustman and F. Kerze, Metallurgy of Zirconium, National Nuclear Energy Series, Division VII 4, 1st Edition, 1955, Mc Graw-Hill, New York
5. W.L. Mudge, Jr., "Effect of Hydrogen on the Embrittlement of Zirconium and Zirconium-Tin Alloys," Zirconium and Zirconium Alloys, 1953, p. 146, American Society for Metals.